IEEE Access
Multidisciplinary ⋮ Rapid Review ⋮ Open Access Journal

Received July 27, 2016, accepted August 15, 2016, date of publication August 19, 2016, date of current version February 20, 2017.

Digital Object Identifier 10.1109/ACCESS.2016.2601648

Dual-Mode Index Modulation Aided OFDM

TIANQI MAO[1], (Student Member, IEEE), ZHAOCHENG WANG[1], (Senior Member, IEEE), QI WANG[1], (Member, IEEE), SHENG CHEN[2,3], (Fellow, IEEE), AND LAJOS HANZO[2], (Fellow, IEEE)

[1]Tsinghua National Laboratory for Information Science and Technology, Department of Electronic Engineering, Tsinghua University, Beijing 100084, China
[2]Electronics and Computer Science, University of Southampton, Southampton SO17 1BJ, U.K.
[3]King Abdulaziz University, Jeddah 21589, Saudi Arabia

Corresponding author: L. Hanzo (lh@ecs.soton.ac.uk)

This work was supported in part by the National Key Basic Research Program of China under Grant 2013CB329203, in part by the National Natural Science Foundation of China under Grant 61571267, in part by Shenzhen Peacock Plan under Grant 1108170036003286, and in part by the Shenzhen Visible Light Communication System Key Laboratory under Grant ZDSYS20140512114229398.

ABSTRACT Index modulation has become a promising technique in the context of orthogonal frequency division multiplexing (OFDM), whereby the specific activation of the frequency domain subcarriers is used for implicitly conveying extra information, hence improving the achievable throughput at a given bit error ratio (BER) performance. In this paper, a dual-mode OFDM technique (DM-OFDM) is proposed, which is combined with index modulation and enhances the attainable throughput of conventional index-modulation-based OFDM. In particular, the subcarriers are divided into several subblocks, and in each subblock, all the subcarriers are partitioned into two groups, modulated by a pair of distinguishable modem-mode constellations, respectively. Hence, the information bits are conveyed not only by the classic constellation symbols, but also implicitly by the specific activated subcarrier indices, representing the subcarriers' constellation mode. At the receiver, a maximum likelihood (ML) detector and a reduced-complexity near optimal log-likelihood ratio-based detector are invoked for demodulation. The minimum distance between the different legitimate realizations of the OFDM subblocks is calculated for characterizing the performance of DM-OFDM. Then, the associated theoretical analysis based on the pairwise error probability is carried out for estimating the BER of DM-OFDM. Furthermore, the simulation results confirm that at a given throughput, DM-OFDM achieves a considerably better BER performance than other OFDM systems using index modulation, while imposing the same or lower computational complexity. The results also demonstrate that the performance of the proposed low-complexity detector is indistinguishable from that of the ML detector, provided that the system's signal to noise ratio is sufficiently high.

INDEX TERMS Orthogonal frequency division multiplexing (OFDM), index modulation, index pattern, constellation, maximum likelihood detection, log-likelihood ratio based detection.

I. INTRODUCTION

Orthogonal frequency division multiplexing (OFDM) has become a ubiquitous digital communications technique as a benefit of its numerous virtues, including its capability of providing high-rate data transmission by splitting the serial data into many low-rate parallel data streams [1]. It is also capable of offering a low-complexity high-performance solution for mitigating the inter-symbol interference (ISI) caused by a dispersive channel [2], [3]. Due to the above-mentioned merits, OFDM has been adopted in many broadband wireless standards, such as 802.11a/g Wi-Fi, 802.16 WiMAX, and Long-Term Evolution (LTE) [1].

The concept of index modulation (IM) is related to the principle of spatial modulation [4]–[6] originally conceived for multiple-input-multiple-output (MIMO) systems, which was then also invoked in the context of OFDM, leading to the index-modulation-based OFDM philosophy. Explicitly, the information is transmitted using both the classic amplitude as well as phase modulation and implicitly also by the indices of the activated subcarriers [7]–[9]. Index-modulation-based OFDM is capable of enhancing the power efficiency of the classic OFDM, since only a fraction of the subcarriers is modulated, but additional information bits are transmitted by mapping them to the subcarrier domain. Hence various attractive IM-aided OFDM systems have been proposed in the literature. In [10], the specific choice of the activated subcarrier indices conveys extra information in an on-off keying (OOK) fashion, whereby the indices of the activated subcarriers are determined by the corresponding majority bit-values of the OOK data streams. Whilst it is capable

of attaining a high power efficiency, this scheme imposes a potential bit error propagation, hence leading to bursts of errors. To address this problem, an enhanced subcarrier index modulation OFDM (ESIM-OFDM) scheme was proposed in [11], where each bit of the OOK data streams determines the active subcarrier in a corresponding subcarrier pair, thus only half of the subcarriers are modulated. Although this scheme is capable of enhancing the attainable performance, constellations of higher order are required for modulation in order to achieve the same spectral efficiency as conventional OFDM.

Basar *et al.* [12] combined OFDM with index modulation (OFDM-IM) by arranging for the subcarriers to be partitioned into several subblocks, where the specific indices of the active subcarriers in each subblock are used for data transmission. This OFDM-IM scheme is capable of enhancing the bit error ratio (BER) performance of classical OFDM at the cost of a reduced throughput, since many subcarriers remain unmodulated in order to implicitly convey information. In [13] Basar proposed an enhanced version of OFDM-IM by combining space-time block codes with coordinate interleaving and OFDM-IM, which led to an additional diversity gain. OFDM-IM was also combined by Basar [14] with the MIMO concept, which led to the MIMO-OFDM-IM philosophy, exhibiting a considerable performance gain over classical MIMO-OFDM [15]. Besides, in [16] and [17], the OFDM-IM scheme is introduced to the underwater acoustic communications as well as the vehicle-to-vehicle and vehicle-to-infrastructure (V2X) applications, which achieves significant performance gains. Furthermore, the performance trade-offs of OFDM-IM techniques have been theoretically analyzed in [18]–[21]. Specifically, in [18], a tight BER upper-bound of OFDM-IM was formulated, and the optimal number of active subcarriers was considered in [19] and [20]. In [21], the achievable performance of OFDM-IM and the beneficial region of the OFDM-IM scheme over conventional OFDM are investigated, which provides the guidelines for system designing of the OFDM-IM scheme. Additionally, several feasible improvements on the performance of OFDM-IM have been discussed in [22] and [23]. Yang *et al.* [22] proposed a spectrum-efficient index modulation scheme with improved mapping, allowing each OFDM subblock to use different constellations and different number of active subcarriers to ehance the spectral efficiency. While Zheng *et al.* [23] concentrated on the transceiver design of the OFDM with in-phase/quadrature index modulation (OFDM-I/Q-IM), which employs both the in-phase and the quadrature components of signals for index modulation. However, the critical problem of throughput loss has not been addressed in the open literature.

Against this background, in this paper, a dual-mode OFDM relying on index modulation (DM-OFDM) is proposed, where all the subcarriers are modulated, which enhances the spectral efficiency of the existing OFDM-IM techniques. In our DM-OFDM scheme the subcarriers are partitioned into OFDM subblocks, and for each subblock, information bits are transmitted not only by the modulated subcarriers but implicitly also by the indices of the activated subcarriers. More specifically, the subcarriers are split into two groups, corresponding to two index subsets. Both groups of subcarriers are then modulated by two different constellation modes, and the information bits conveyed by index modulation can be determined by one of the two index subsets. At the receiver, a maximum likelihood (ML) detector and a reduced-complexity near optimal log-likelihood ratio (LLR) detector are employed to demodulate the signals. The minimum distance between the different realizations of the OFDM subblocks is calculated in order to evaluate the BER performance of DM-OFDM with the aid of the ML detector. Explicitly, the theoretical analysis is based on the pairwise error probability (PEP) of the proposed DM-OFDM. Our simulation results will demonstrate that DM-OFDM achieves a signal to noise ratio (SNR) gain of several dBs over OFDM-IM both in additive white Gaussian noise (AWGN) channels and in frequency-selective Rayleigh fading channel at the spectral efficiency of 4 bits/s/Hz, while imposing the same or lower computational complexity. Our simulation results will also confirm that the performance of the low-complexity LLR based detector is indistinguishable from that of the ML detector, provided that the system's SNR is sufficiently high.

The rest of this paper is organized as follows. Section II describes the system model of DM-OFDM, while Section III presents our theoretical analysis of the proposed DM-OFDM. Section IV calculates the minimum distance between different OFDM subblocks, performs the PEP analysis, and carries out Monte Carlo simulations for quantifying the performance of the proposed DM-OFDM, using the existing OFDM-IM as a benchmark. Finally, our conclusions are drawn in Section V.

II. DM-OFDM SYSTEM MODEL

A. DM-OFDM TRANSMITTER AND CHANNEL MODEL

The DM-OFDM transmitter is illustrated in Fig. 1. First, m incoming bits are partitioned by a bit splitter into p groups, each consisting of g bits, i.e., $p = m/g$. Each group of g information bits is fed into an index selector and two different constellation mappers for generating an OFDM subblock of length $l = N/p$, where N is the size of fast Fourier transform (FFT). In contrast to the existing index-modulation-based OFDM [12], whereby only part of the subcarriers are actively modulated, in our DM-OFDM scheme all the subcarriers are modulated in each subblock, which leads to an enhanced spectral efficiency. The first g_1 bits of the incoming g bits, referred as index bits, are utilized by the index selector to divide the indices of each subblock into two index subsets, denoted as $\mathcal{I}_A$ and $\mathcal{I}_B$. The remaining g_2 bits are passed to the mappers A and B having the constellation sets of $\mathcal{M}_A$ and $\mathcal{M}_B$ associated with the sizes M_A and M_B, respectively, where we have $\mathcal{M}_A \wedge \mathcal{M}_B = \varnothing$. With the aid of the index selector, the subcarriers corresponding to $\mathcal{I}_A$ and $\mathcal{I}_B$ are modulated by the mappers A and B, respectively. Assuming that k subcarriers of a subblock are modulated

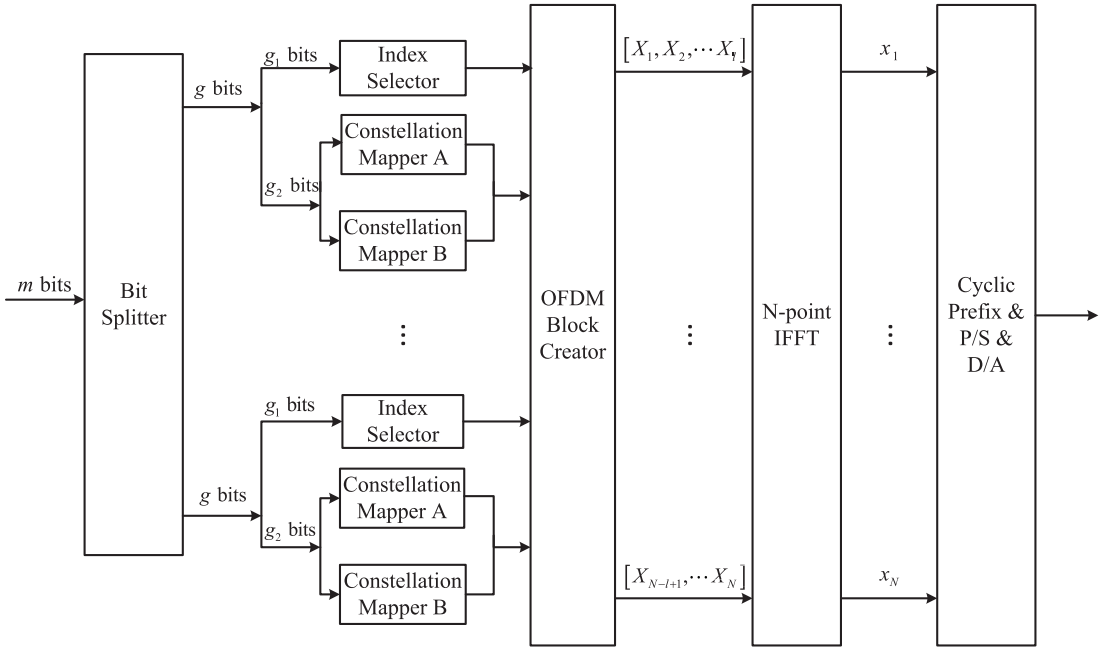

FIGURE 1. System model of the DM-OFDM transmitter.

TABLE 1. A Look-Up Table of Index Modulation For $g_1 = 2$, $l = 4$, and $k = 2$.

Index bits	Indices	Subblocks
[0, 0]	[1, 2]	$[S_A^{(1)}, S_A^{(2)}, S_B^{(1)}, S_B^{(2)}]$
[0, 1]	[2, 3]	$[S_B^{(1)}, S_A^{(1)}, S_A^{(2)}, S_B^{(2)}]$
[1, 0]	[3, 4]	$[S_B^{(1)}, S_B^{(2)}, S_A^{(1)}, S_A^{(2)}]$
[1, 1]	[1, 4]	$[S_A^{(1)}, S_B^{(1)}, S_B^{(2)}, S_A^{(2)}]$

with $\mathcal{M}_A$, while the other $(l-k)$ subcarriers are modulated with $\mathcal{M}_B$, then g_1 and g_2 can be calculated respectively according to

$$g_1 = \left\lfloor \log_2 \left(\frac{l!}{(l-k)!k!} \right) \right\rfloor, \tag{1}$$

$$g_2 = k \log_2(M_A) + (l-k) \log_2(M_B), \tag{2}$$

where $\lfloor\ \rfloor$ denotes the integer floor operator.

Once $\mathcal{I}_A$ is known, $\mathcal{I}_B$ is also determined. Hence we only have to define $\mathcal{I}_A$ for the index selector. Clearly, there are $n_I = 2^{g_1}$ distinctive index patterns, which are given by the index set

$$\mathcal{I}_A \in \left\{ \mathbf{I}_A^{(1)}, \mathbf{I}_A^{(2)}, \cdots, \mathbf{I}_A^{(n_I)} \right\}. \tag{3}$$

The operations of the index selector are exemplified by Table 1, where we have $g_1 = 2$, $l = 4$, and $k = 2$. For each subblock, the indices of the subcarriers modulated by the mapper A are determined by the two index bits, which assume the values of [0, 0], [0, 1], [1, 0] and [1, 1], as $\mathbf{I}_A^{(1)} = [1, 2]$, $\mathbf{I}_A^{(2)} = [2, 3]$, $\mathbf{I}_A^{(3)} = [3, 4]$ and $\mathbf{I}_A^{(4)} = [1, 4]$, while the other subcarriers are modulated by the mapper B. In order to reliably detect the index pattern

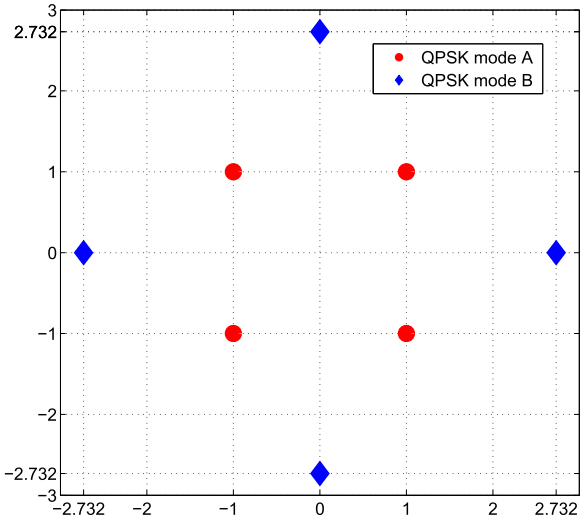

FIGURE 2. An example of DM-OFDM constellation design for $\mathcal{M}_A$ and $\mathcal{M}_B$ with $M_A = M_B = 4$.

at the receiver, the constellations generated by the mappers A and B should be readily differentiable, namely, we have to have $\mathcal{M}_A \wedge \mathcal{M}_B = \varnothing$. For example, if quadrature phase shift keying (QPSK) is employed by both mappers, a feasible constellation design is illustrated in Fig. 2. Specifically, an 8-level quadrature amplitude modulation (QAM) constellation is employed, whereby the two sets $\mathcal{M}_A = \{-1-\mathbf{j}, 1-\mathbf{j}, 1+\mathbf{j}, -1+\mathbf{j}\}$ and $\mathcal{M}_B = \{1+\sqrt{3}, (1+\sqrt{3})\mathbf{j}, -1-\sqrt{3}, -(1+\sqrt{3})\mathbf{j}\}$ are defined as the inner QPSK and the outer QPSK, respectively. The inner QPSK schemes is associated with mapper A, while the outer one with mapper B. In gen-

eral, given an $(M_A + M_B)$-QAM constellation, arbitrary M_A constellation points can be employed by the mapper A, which are denoted by the set

$$\mathcal{M}_A = \{S_A(j) : 1 \le j \le M_A\}, \tag{4}$$

and the other M_B constellation points are employed by the mapper B which are denoted by

$$\mathcal{M}_B = \{S_B(j) : 1 \le j \le M_B\}. \tag{5}$$

After the mapping, an N-point inverse FFT (IFFT) operation is performed following the concatenation of the p different OFDM subblocks

$$\begin{aligned}\mathbf{X}^{(\beta)} &= \left[X_{(\beta-1)l+1}\, X_{(\beta-1)l+2} \cdots X_{\beta l}\right]^T \\ &= \left[X_1^{(\beta)}\, X_2^{(\beta)} \cdots X_l^{(\beta)}\right]^T,\ 1 \le \beta \le p,\end{aligned} \tag{6}$$

to generate the time-domain (TD) signals $\mathbf{x} = \left[x_1\, x_2 \cdots x_N\right]^T$, where $(\,)^T$ denotes the transpose operator. Next the cyclic prefix (CP) of length L is added, and the resultant signals are then fed into a parallel-to-serial converter (P/S) and a digital-to-analog converter (D/A) to generate the transmit signals. Finally, the outputs of the transmitter are transmitted through a frequency-selective Rayleigh fading channel whose channel impulse response (CIR) length v is no higher than the CP length of L. The TD CIR coefficient vector is given by $\mathbf{h} = \left[h_1\, h_2 \cdots h_v\right]^T$, where each h_i, $1 \le i \le v$, is a circularly symmetric complex Gaussian random variable following the distribution of $\mathcal{CN}\left(0, \frac{1}{v}\right)$ [12]. The frequency domain channel transfer function coefficients (FDCTFCs), defined as the N-point FFT of $\mathbf{h}$, can be represented by

$$\mathbf{H} = \left[H_1\, H_2 \cdots H_N\right]^T = \frac{1}{\sqrt{N}}\mathrm{FFT}\left(\overline{\mathbf{h}}\right), \tag{7}$$

where the N-dimensional vector $\overline{\mathbf{h}} = \left[h_1\, h_2 \cdots h_v\, 0 \cdots 0\right]^T$, and $\frac{1}{\sqrt{N}}\mathrm{FFT}(\,)$ denotes the N-point FFT operator.

At the receiver, after the CP removal, the channel-impaired and noise-contaminated received signals are passed to the N-point FFT processor to yield the frequency-domain (FD) received signal vector $\mathbf{Y} = \left[Y_1\, Y_2 \cdots Y_N\right]^T$, which satisfies

$$Y_n = H_n X_n + W_n,\ 1 \le n \le N, \tag{8}$$

where W_n is the FD representation of the AWGN with power N_0. In particular, for the βth OFDM subblock, where $1 \le \beta \le p$, we have

$$\mathbf{Y}^{(\beta)} = \mathrm{diag}\left\{\mathbf{X}^{(\beta)}\right\}\mathbf{H}^{(\beta)} + \mathbf{W}^{(\beta)}, \tag{9}$$

where $\mathrm{diag}\left\{\mathbf{X}^{(\beta)}\right\}$ is the diagonal matrix with its diagonal elements given by the elements of $\mathbf{X}^{(\beta)}$, while

$$\begin{aligned}\mathbf{Y}^{(\beta)} &= \left[Y_{(\beta-1)l+1}\, Y_{(\beta-1)l+2} \cdots Y_{\beta l}\right]^T \\ &= \left[Y_1^{(\beta)}\, Y_2^{(\beta)} \cdots Y_l^{(\beta)}\right]^T,\end{aligned} \tag{10}$$

$$\begin{aligned}\mathbf{H}^{(\beta)} &= \left[H_{(\beta-1)l+1}\, H_{(\beta-1)l+2} \cdots H_{\beta l}\right]^T \\ &= \left[H_1^{(\beta)}\, H_2^{(\beta)} \cdots H_l^{(\beta)}\right]^T,\end{aligned} \tag{11}$$

$$\begin{aligned}\mathbf{W}^{(\beta)} &= \left[W_{(\beta-1)l+1}\, W_{(\beta-1)l+2} \cdots W_{\beta l}\right]^T \\ &= \left[W_1^{(\beta)}\, W_2^{(\beta)} \cdots W_l^{(\beta)}\right]^T.\end{aligned} \tag{12}$$

Given each index pattern $\mathbf{I}_A^{(i)} \in \mathcal{I}_A$, there are $n_S = M_A^k M_B^{(l-k)}$ legitimate transmit signal vectors for $\mathbf{X}^{(\beta)}$, which is defined by the set

$$\mathcal{S}_{\mathbf{I}_A^{(i)}} = \left\{\mathbf{S}_{\mathbf{I}_A^{(i)}}^{(1)}, \mathbf{S}_{\mathbf{I}_A^{(i)}}^{(2)}, \cdots, \mathbf{S}_{\mathbf{I}_A^{(i)}}^{(n_S)}\right\}. \tag{13}$$

Each $\mathbf{S}_{\mathbf{I}_A^{(i)}}^{(j)} \in \mathcal{S}_{\mathbf{I}_A^{(i)}}$ is an l-dimensional vector $\mathbf{S}_{\mathbf{I}_A^{(i)}}^{(j)} = \left[S_{\mathbf{I}_A^{(i)}}^{(j)}(1)\, S_{\mathbf{I}_A^{(i)}}^{(j)}(2) \cdots S_{\mathbf{I}_A^{(i)}}^{(j)}(l)\right]^T$. Thus, there are a total of $n_X = n_I n_S = 2^{g_1} M_A^k M_B^{(l-k)}$ legitimate transmit signal vectors for $\mathbf{X}^{(\beta)}$.

It is indicated that the spectral efficiency of the proposed DM-OFDM can be calculated as $\frac{p(g_1+g_2)}{N+L}$. According to (1) and (2), the spectral efficiency can be further improved by enlarging the subblock size l. Assuming N is fixed, then the total number of transmitted bits conveyed by index modulation becomes $n_{IM} = \lfloor N/l \rfloor \left\lfloor \log_2 \binom{l}{k} \right\rfloor$. To maximize n_{IM} for a fixed l, k is set as $l/2$ according to the innate property of the combinatorial expression. It is indicated that n_{IM} increases as l becomes larger, leading to an improved spectral efficiency for DM-OFDM. However, the computational complexity of the brute-force ML detector is increased exponentially with the size of the OFDM subblocks. Therefore, a trade-off has to be struck between the spectral efficiency and the computational complexity in order to optimize the overall performance of DM-OFDM, which is set aside for our future work.

B. ML DETECTOR FOR DM-OFDM

At the receiver, a full ML detector may be invoked for detecting the information bits by processing the FD received signals on a subblock by subblock manner. For the βth subblock, the optimal index pattern and transmitted symbols can be obtained by minimizing the ML metric

$$\left\{\mathbf{I}_A^{(i^*)}, \mathbf{S}_{\mathbf{I}_A^{(i^*)}}^{(j^*)}\right\} = \arg \min_{\mathbf{I}_A^{(i)} \in \mathcal{I}_A, \mathbf{S}_{\mathbf{I}_A^{(i)}}^{(j)} \in \mathcal{S}_{\mathbf{I}_A^{(i)}}} \sum_{k=1}^{l} \left| Y_k^{(\beta)} - H_k^{(\beta)} S_{\mathbf{I}_A^{(i)}}^{(j)}(k) \right|^2. \tag{14}$$

After obtaining the ML estimate of both the index pattern and of the symbol vector $\left\{\mathbf{I}_A^{(i^*)}, \mathbf{S}_{\mathbf{I}_A^{(i^*)}}^{(j^*)}\right\}$, the $g = g_1 + g_2$ information bits can be demodulated by employing the index-pattern look-up table and the two constellation sets, which map the information bits to the corresponding index pattern and to the constellation symbols. It can be seen from (14) that the computational complexity of the ML detector in terms of complex multiplications is on the order of $2^{g_1} M_A^k M_B^{(l-k)}$ per subblock, denoted as $\mathcal{O}\left(2^{g_1} M_A^k M_B^{(l-k)}\right)$. Therefore, the ML detector is impractical to implement for large g_1, l, k and modulation orders M_A and M_B, due to its exponentially increasing complexity.

C. REDUCED-COMPLEXITY LLR DETECTOR FOR DM-OFDM

To reduce the detection complexity, we propose an LLR based detector for DM-OFDM. Since each subcarrier is modulated by either the mapper A or the mapper B, the constellation mode of each subcarrier can be obtained by calculating the logarithm of the ratio between the *a posteriori* probabilities of the subcarrier being modulated by the mapper A and by the mapper B, respectively, which is formulated as

$$\gamma_n = \ln\left(\frac{\sum_{j=1}^{M_A}\Pr\left(X_n = S_A(j)|Y_n\right)}{\sum_{q=1}^{M_B}\Pr\left(X_n = S_B(q)|Y_n\right)}\right), \tag{15}$$

where $1 \le n \le N$, $S_A(j) \in \mathcal{M}_A$ and $S_B(q) \in \mathcal{M}_B$. It can be seen from (15) that the nth subcarrier is more likely to be modulated by the mapper A if γ_n is positive, and more likely to be modulated by the mapper B if γ_n is negative. Since $\sum_{j=1}^{M_A}\Pr\left(X_n = S_A(j)\right) = k/l$ and $\sum_{q=1}^{M_B}\Pr\left(X_n = S_B(q)\right) = (l-k)/l$, using Bayes rule, (15) can be further expressed as

$$\begin{aligned}\gamma_n =& \ln\left(\frac{M_B k}{M_A(l-k)}\right) + \ln\left(\sum_{j=1}^{M_A}\exp\left(-\frac{1}{N_0}\left|Y_n - H_n S_A(j)\right|^2\right)\right)\\ &- \ln\left(\sum_{q=1}^{M_B}\exp\left(-\frac{1}{N_0}\left|Y_n - H_n S_B(q)\right|^2\right)\right).\end{aligned} \tag{16}$$

To avoid potential computation overflow, the Jacobian logarithm [24], [25] is used for calculating the terms $\ln\left(\sum_{j=1}^{M_A}\exp\left(-\frac{1}{N_0}\left|Y_n - H_n S_A(j)\right|^2\right)\right)$ and $\ln\left(\sum_{q=1}^{M_B}\exp\left(-\frac{1}{N_0}\left|Y_n - H_n S_B(q)\right|^2\right)\right)$. Consider the first term as an example, while the other term can be calculated in the same way. We define $\lambda_j = -\frac{1}{N_0}\left|Y_n - H_n S_A(j)\right|$ for $j = 1, 2, \cdots, M_A$. The recursion is initialized by

$$\begin{aligned}\ln\left(e^{\lambda_1} + e^{\lambda_2}\right) &= \max\{\lambda_1, \lambda_2\} + \ln\left(1 + e^{-|\lambda_2 - \lambda_1|}\right)\\ &= \max\{\lambda_1, \lambda_2\} + f\left(|\lambda_1 - \lambda_2|\right),\end{aligned} \tag{17}$$

where $f(\,)$ is known as the correction function. Then given $\Delta = \ln\left(e^{\lambda_1} + e^{\lambda_2} + \cdots + e^{\lambda_{\chi-1}}\right)$ for $\chi = 2, 3, \cdots, M_A$, we have

$$\begin{aligned}&\ln\left(e^{\lambda_1} + e^{\lambda_2} + \cdots + e^{\lambda_\chi}\right)\\ &= \ln\left(e^{\Delta} + e^{\lambda_\chi}\right)\\ &= \max\{\Delta, \lambda_\chi\} + \ln\left(1 + e^{-|\lambda_\chi - \Delta|}\right)\\ &= \max\{\Delta, \lambda_\chi\} + f(|\Delta - \lambda_\chi|).\end{aligned} \tag{18}$$

By applying (18) iteratively from $\chi = 2$ to M_A, $\ln\left(\sum_{j=1}^{M_A}\exp\left(-\frac{1}{N_0}\left|Y_n - H_n S_A(j)\right|^2\right)\right)$ is calculated. Hence, the LLR value of γ_n can be obtained using Algorithm 1.

After obtaining the signs of γ_n, i.e., $\bar{\gamma}_n = \mathrm{sgn}(\gamma_n)$, for $1 \le n \le N$, we can group them into the p blocks as

$$\begin{aligned}\bar{\boldsymbol{\gamma}}^{(\beta)} &= \left[\bar{\gamma}_{(\beta-1)l+1}\ \bar{\gamma}_{(\beta-1)l+2}\cdots\bar{\gamma}_{\beta l}\right]^T\\ &= \left[\bar{\gamma}_1^{(\beta)}\ \bar{\gamma}_2^{(\beta)}\cdots\bar{\gamma}_l^{(\beta)}\right]^T,\ 1 \le \beta \le p.\end{aligned} \tag{19}$$

Algorithm 1 Iterative LLR Calculation for DM-OFDM

Require: Received signals Y_n, FDCTFCs H_n, noise energy N_0, constellation sets $\mathcal{M}_A$ and $\mathcal{M}_B$, and their sizes M_A and M_B, size of OFDM subblock l, number of subcarriers modulated by mapper A per subblock k;

Ensure: γ_n is LLR of nth subcarrier;

```
Δ1 = −(1/N0)|Yn − Hn SA(1)|^2;
Δ2 = −(1/N0)|Yn − Hn SB(1)|^2;
for (j = 2; j ≤ MA; j++) do
    T1 = −(1/N0)|Yn − Hn SA(j)|^2;
    T2 = max{Δ1, T1} + f(|Δ1 − T1|);
    Δ1 = T2;
end for
for (q = 2; q ≤ MB; q++) do
    T1 = −(1/N0)|Yn − Hn SB(q)|^2;
    T2 = max{Δ2, T1} + f(|Δ2 − T1|);
    Δ2 = T2;
end for
γn = ln(k) − ln(l − k) + Δ1 − Δ2;
return γn;
```

Since $\bar{\boldsymbol{\gamma}}^{(\beta)}$ indicates which subcarriers of the βth subblock are modulated by the mapper A and which subcarriers are modulated by the mapper B, it is equivalent to the index pattern. Thus, $\bar{\boldsymbol{\gamma}}^{(\beta)}$ can be utilized to demodulate the corresponding g_1 index bits according to the index pattern look-up table. Furthermore, since $\bar{\gamma}_i^{(\beta)}$ for $1 \le i \le l$ indicates whether $X_i^{(\beta)}$ is modulated by the mapper A or by the mapper B, the ML estimate for $X_i^{(\beta)}$ is given by

$$\widehat{X}_i^{(\beta)} = \begin{cases}\arg\min\limits_{S_A(j)\in\mathcal{M}_A}\left|Y_i^{(\beta)} - H_i^{(\beta)} S_A(j)\right|^2, & \bar{\gamma}_l^{(\beta)} = +1,\\ \arg\min\limits_{S_B(j)\in\mathcal{M}_B}\left|Y_i^{(\beta)} - H_i^{(\beta)} S_B(j)\right|^2, & \bar{\gamma}_l^{(\beta)} = -1,\end{cases} \tag{20}$$

where $1 \le i \le l$. This yields the g_2 estimated information bits for subblock β.

Remark: Under an extremely high noisy condition, it is possible that a $\bar{\boldsymbol{\gamma}}^{(\beta)}$ obtained may not correspond to a legitimate index pattern. In such a situation, a solution is to reverse the sign of the LLR having the smallest magnitude in the subblock to see if a legitimate index pattern can be inferred. If the resultant modified $\bar{\boldsymbol{\gamma}}^{(\beta)}$ is still illegitimate, the LLR with the second smallest magnitude can be examined, and so on until a legitimate index pattern is produced [26].

This LLR based detector is clearly a near-ML solution. However, its computational complexity is much lower than that of the ML detector. Specifically, the complexity of calculating the LLRs for a subblock is on the order of $\mathcal{O}\left(l(M_A + M_B)\right)$ in terms of complex multiplications, while the complexity of performing the ML demodulation for a subblock given index pattern is on the order of $\mathcal{O}\left(kM_A + (l-k)M_B\right)$. Therefore, the complexity of this LLR based detector is on the order of $\mathcal{O}\left(l(M_A + M_B)\right)$ per subblock in terms of complex multiplications. Moreover, in an

environment having a sufficiently high SNR, the performance of this LLR detector is indistinguishable from that of the ML detector. Thus the LLR based detector is a better choice for practical DM-OFDM systems.

Recently, a novel reduced-complexity receiver was proposed for the detection of index-modulated OFDM in [27]. Since there is still slight performance gap between the proposed LLR detector and the ML detector at low SNRs, the reduced-complexity detector in [27] will be also applied in DM-OFDM in our future study, which may harvest on performance gain over the proposed low-complexity LLR detector.

III. PERFORMANCE ANALYSIS OF DM-OFDM

According to (14), the performance of DM-OFDM relying on the ML detector is determined by the minimum distance between the different realizations of the OFDM subblock. First, let us define the set of n_X realizations for the OFDM subblock by

$$\mathcal{X}_{sb} = \left\{ \mathbf{X}_{(i,j)} = \mathbf{S}^{(j)}_{\mathbf{I}^{(i)}_A} : \forall \mathbf{I}^{(i)}_A \in \mathcal{I}_A, \mathbf{S}^{(j)}_{\mathbf{I}^{(i)}_A} \in \mathcal{S}_{\mathbf{I}^{(i)}_A} \right\}, \quad (21)$$

and let us denote the l-dimensional realization vector by $\mathbf{X}_{(i,j)} = \left[X_{(i,j)}(1)\ X_{(i,j)}(2) \cdots X_{(i,j)}(l)\right]^T$. The distance metric between two different realization vectors $\mathbf{X}_{(i_1,j_1)}$ and $\mathbf{X}_{(i_2,j_2)}$ is given by

$$D(\mathbf{X}_{(i_1,j_1)}, \mathbf{X}_{(i_2,j_2)}) = \sqrt{\sum_{t=1}^{l} \left| X_{(i_1,j_1)}(t) - X_{(i_2,j_2)}(t) \right|^2}. \quad (22)$$

Therefore, the minimum distance normalized by the transmitted bit energy, denoted as $d_{\min}$, can be formulated as

$$d_{\min} = \min_{\mathbf{X}_{(i_1,j_1)}, \mathbf{X}_{(i_2,j_2)} \in \mathcal{X}_{sb} \ \forall (i_1,j_1) \neq (i_2,j_2)} \sqrt{\frac{1}{E_b} D\left(\mathbf{X}_{(i_1,j_1)}, \mathbf{X}_{(i_2,j_2)}\right)}, \quad (23)$$

where $E_b = E_s(N+L)/m = (E_s(N+L))\,/\,(p(g_1+g_2))$ is the average transmitted energy per bit of DM-OFDM, and E_s denotes the average transmitted symbol energy.

The performance metric of $d_{\min}$ can also be applied to OFDM-IM if the same ML detector is utilized. Therefore, we can employ the minimum distance of the OFDM subblock as a metric to evaluate the performance of both the DM-OFDM and OFDM-IM.

The performance of DM-OFDM using the ML detector can be also estimated by PEP analysis. Since the PEP events in different subblocks are identical [12], analyzing a single OFDM subblock is sufficient. The received signal for the generic βth subblock is given in (9). For notational convenience, we denote $\mathbf{X}_{diag} = \text{diag}\{\mathbf{X}^{(\beta)}\}$. The conditioned pairwise error probability (CPEP) of the event that the transmitted $\mathbf{X}_{diag}$ is detected as $\widehat{\mathbf{X}}_{diag}$ is given by [12]

$$\Pr\left(\mathbf{X}_{diag} \to \widehat{\mathbf{X}}_{diag} | \mathbf{H}^{(\beta)}\right) = Q\left(\sqrt{\frac{E_s \eta}{2N_0}}\right), \quad (24)$$

where $Q(\,)$ is the Gaussian Q-function, and

$$\eta = \left\| \left(\mathbf{X}_{diag} - \widehat{\mathbf{X}}_{diag}\right) \mathbf{H}^{(\beta)} \right\|_F^2 = \left(\mathbf{H}^{(\beta)}\right)^H \mathbf{\Gamma} \mathbf{H}^{(\beta)} \quad (25)$$

in which $(\,)^H$ denotes the conjugate transpose operator and $\mathbf{\Gamma} = \left(\mathbf{X}_{diag} - \widehat{\mathbf{X}}_{diag}\right)^H \left(\mathbf{X}_{diag} - \widehat{\mathbf{X}}_{diag}\right)$. According to [28], (24) can be approximated as

$$\Pr\left(\mathbf{X}_{diag} \to \widehat{\mathbf{X}}_{diag} | \mathbf{H}^{(\beta)}\right) \approx \frac{1}{12} \exp\left(-\frac{E_s \eta}{4N_0}\right) + \frac{1}{4} \exp\left(-\frac{E_s \eta}{3N_0}\right). \quad (26)$$

Then the corresponding unconditioned pairwise error probability (UPEP) is formulated as

$$\Pr\left(\mathbf{X}_{diag} \to \widehat{\mathbf{X}}_{diag}\right) \approx E_{\mathbf{H}^{(\beta)}} \left\{ \frac{1}{12} \exp\left(-\frac{E_s \eta}{4N_0}\right) + \frac{1}{4} \exp\left(-\frac{E_s \eta}{3N_0}\right) \right\}, \quad (27)$$

where $E_{\mathbf{H}^{(\beta)}}\{\,\}$ denotes the expectation operation with respect to $\mathbf{H}^{(\beta)}$. The correlation matrix of $\mathbf{H}^{(\beta)}$ is defined by $\mathbf{C} = E\left\{\mathbf{H}^{(\beta)}\left(\mathbf{H}^{(\beta)}\right)^H\right\}$. According to [29], $\mathbf{C}$ can be decomposed as $\mathbf{Q}\mathbf{\Lambda}\mathbf{Q}^H$, whereby $\mathbf{H}^{(\beta)} = \mathbf{Q}\mathbf{v}$ with $\Lambda = E\left\{\mathbf{v}\mathbf{v}^H\right\}$. Then the probability density function (PDF) of the stochastic vector $\mathbf{v}$ can be derived as

$$f(\mathbf{v}) = \frac{\pi^{-r}}{\det(\Lambda)} \exp\left(-\mathbf{v}^H \Lambda^{-1} \mathbf{v}\right), \quad (28)$$

where r is the rank of $\mathbf{C}$, and det( ) denotes the determinant operator. Applying (28) to complete the expectation operation in (27) yields the following expression of $\Pr\left(\mathbf{X}_{diag} \to \widehat{\mathbf{X}}_{diag}\right)$ [12]

$$\Pr\left(\mathbf{X}_{diag} \to \widehat{\mathbf{X}}_{diag}\right) \approx \frac{1}{12 \det\left(\mathbf{I}_l + \frac{E_s}{4N_0}\mathbf{C}\mathbf{\Gamma}\right)} + \frac{1}{4 \det\left(\mathbf{I}_l + \frac{E_s}{3N_0}\mathbf{C}\mathbf{\Gamma}\right)}, \quad (29)$$

where $\mathbf{I}_l$ denotes the $l \times l$ identity matrix. After the calculation of the UPEP, the average bit error probability (ABEP) can be derived as [12]

$$P_{ave} = \frac{1}{g n_X} \sum_{\mathbf{X}_{diag} \neq \widehat{\mathbf{X}}_{diag}} \Pr\left(\mathbf{X}_{diag} \to \widehat{\mathbf{X}}_{diag}\right) \varepsilon\left(\mathbf{X}_{diag}, \widehat{\mathbf{X}}_{diag}\right), \quad (30)$$

where $\varepsilon\left(\mathbf{X}_{diag}, \widehat{\mathbf{X}}_{diag}\right)$ is the number of bit errors in the corresponding pairwise error event. P_{ave} is approximately equal to the system's BER, and therefore it can be used to estimate the performance of DM-OFDM.

Although the PEP analysis presented here is based on the ML detection, the result of the approximate BER given above can also be applied to the DM-OFDM relying on the LLR based detector, especially under high-SNR conditions. This is because the reduced-complexity LLR based detector offers a near-ML solution, and its performance is indistinguishable from that of the ML detector at high SNRs.

Recently, several improvements based on the conventional OFDM-IM have been proposed [7], [13], [22], [23], which

can be also applied to our proposed DM-OFDM. For example, in [7] and [22] OFDM-IM is generalized by allowing each OFDM subblock to have different number of activated subcarriers and different constellation mappings. And both the quadrature and the in-phase components of signals are employed for index modulation in [7] and [23]. Additionally, coordinate interleaving techniques are used in OFDM-IM by Basar [13]. Since both the proposed DM-OFDM and conventional OFDM-IM divide the subcarriers into OFDM subblocks, and perform index modulation within each subblock, the aforementioned enhancements of OFDM-IM can be readily invoked by DM-OFDM.

IV. NUMERICAL RESULTS

The performance of the proposed DM-OFDM and the existing index-modulation-based OFDM scheme, namely, OFDM-IM, are compared. The frequency-selective Rayleigh fading channel used in the simulation has a CIR length of $v = 10$. The number of subcarriers is set to $N = 128$, divided into $p = 32$ subblocks with 4 subcarriers per subblock, and the length of CP is 16. The system's SNR is defined as E_b/N_0.

Example 1: The constellations of DM-OFDM are depicted in Fig. 2, whereby 2 subcarriers are modulated by the inner QPSK, and the other 2 subcarriers are modulated by the outer QPSK in each OFDM subblock. Hence, a total of $g_1 + g_2 = 2 + 8 = 10$ information bits are transmitted per OFDM subblock, and the spectral efficiency of this DM-OFDM is equal to 2.22 bits/s/Hz. For the OFDM-IM counterpart, 2 subcarriers of each OFDM subblock are modulated by 16-QAM, and the other subcarriers are unmodulated in order to maintain the same spectral efficiency and the same complexity as the DM-OFDM. The $d_{\min}$ metrics for the DM-OFDM and OFDM-IM, denoted as $d_{\min,\mathrm{DM-OFDM}}$ and $d_{\min,\mathrm{OFDM-IM}}$, are 1.3706 and 1.3333, respectively. Since we have $d_{\min,\mathrm{DM-OFDM}} > d_{\min,\mathrm{OFDM-IM}}$, DM-OFDM achieves a better BER performance than its OFDM-IM counterpart for the same spectral efficiency of 2.22 bits/s/Hz.

To validate the above minimum distance based analytical result, the performance comparison of the proposed DM-OFDM and the existing OFDM-IM, both using the ML detector, is carried out by Monte Carlo simulation. The results obtained are shown in Fig. 3. It can be seen from Fig. 3 that at the BER level of 10^{-3}, the proposed DM-OFDM attains 1 dB SNR-gain over OFDM-IM, both for the AWGN and for the frequency-selective Rayleigh fading channels considered. This is because 16-QAM has to be employed in OFDM-IM for reaching the same spectral efficiency as DM-OFDM, which is more sensitive both to noise and to interference. This confirms the above theoretical analysis. In this case, both the DM-OFDM using the ML detector and the OFDM-IM relying on the ML detector have the same computational complexity, which is on the order of $\mathcal{O}(1024)$ per subblock in terms of the number of complex multiplications. Moreover, Fig. 3 characterizes the BER performance of DM-OFDM using the low-complexity LLR based detector. It can be seen that DM-OFDM using the LLR detector only suffers from a slight performance loss compared to the DM-OFDM relying on the ML detector at low SNRs. When the SNR is sufficiently high, the performance of the LLR based detector becomes indistinguishable from that of the ML detector, despite the fact that it imposes a much lower computational complexity than the ML detector, specifically $\mathcal{O}(32)$ in comparison to $\mathcal{O}(1024)$ in this example. Furthermore, the BER performance of DM-OFDM is compared to that of the existing ESIM-OFDM arrangement at the spectral efficiency of 2.22 bits/s/Hz under the AWGN and the frequency-selective Rayleigh fading channel conditions. It can be readily seen that the proposed DM-OFDM regime achieves 1dB and 3dB performance gain over ESIM-OFDM for the AWGN channel and the frequency-selective Rayleigh fading channel respectively, because ESIM-OFDM only activates half of its subcarriers for modulation, hence requiring higher order constellations to reach the spectral efficiency of DM-OFDM, therefore leading to a BER performance loss.

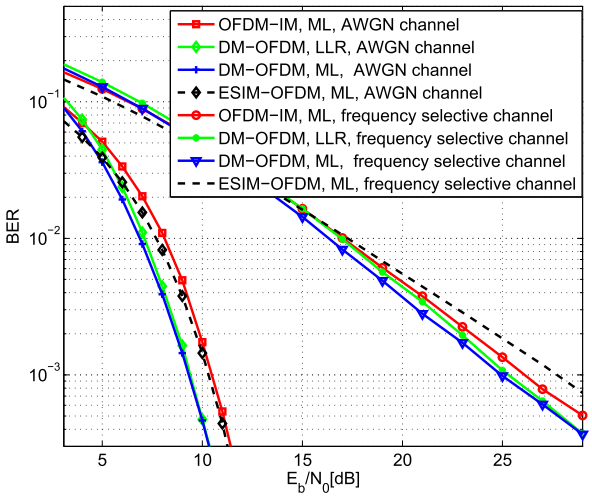

FIGURE 3. Performance comparison between DM-OFDM, OFDM-IM and ESIM-OFDM under both AWGN and frequency-selective Rayleigh fading channel conditions for *Example 1* with the spectral efficiency of 2.22 bits/s/Hz.

Additionally, the theoretical PEP analysis is compared with the simulated BER performance in Fig. 4 for the DM-OFDM under the frequency-selective Rayleigh fading channel considered. At low SNRs, the theoretical analysis becomes inaccurate, because there are several approximations in the PEP calculation, which become inaccurate when the noise is dominant. However, the simulation results agree with the theoretical PEP analysis well when the E_b/N_0 is above 30 dB, indicating that the PEP analysis of DM-OFDM is more accurate at high SNRs.

Besides, Fig. 5 presents the complementary cumulative distribution functions (CCDFs) for the peak-to-average power ratio (PAPR) of the proposed DM-OFDM and the conventional OFDM-IM with values of N, where the subblock length equals 4. For DM-OFDM, two subcarriers are modulated by the outer QPSK of Fig. 2, and the other subcarriers are modulated by the inner QPSK. And for

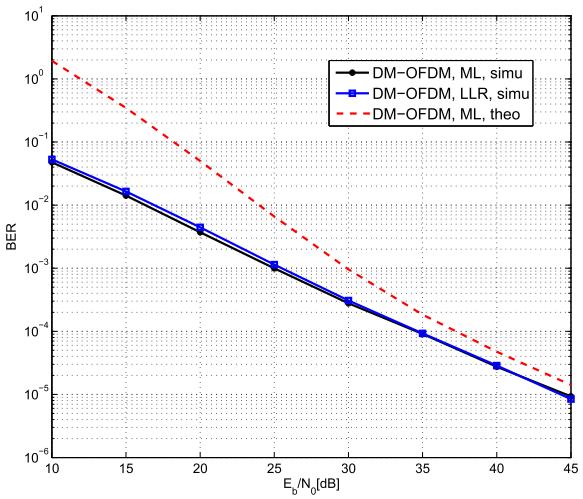

FIGURE 4. Comparison between the theoretical PEP analysis and the simulated BER performances for DM-OFDM under the frequency-selective Rayleigh fading channel of *Example 1*.

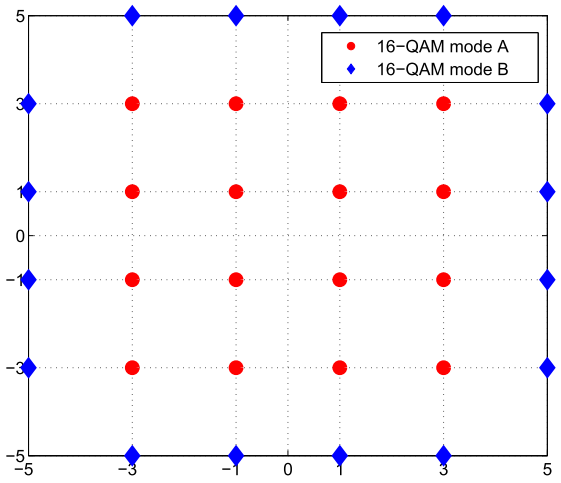

FIGURE 6. DM-OFDM constellation design for $\mathcal{M}_A$ and $\mathcal{M}_B$ with $M_A = M_B = 16$.

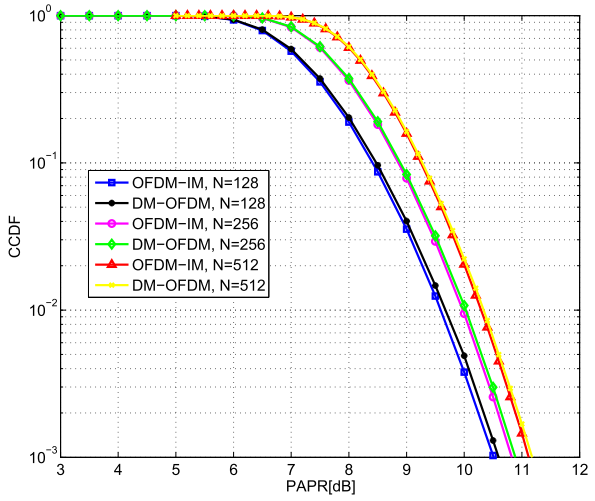

FIGURE 5. the CCDF for PAPR of DM-OFDM and OFDM-IM with N equals 128, 256, and 512.

the OFDM-IM counterpart, two subcarriers of each OFDM subblock are modulated by 16-QAM in order to reach the same spectral efficiency as the proposed DM-OFDM. It can be observed that, when the CCDF equals 10^{-3}, the PAPR of DM-OFDM is almost the same as that of OFDM-IM with $N = 128, 256, 512$. Therefore, although the proposed DM-OFDM may suffer from a slightly higher PAPR than OFDM-IM, the difference can be negligible.

Example 2: The constellations of DM-OFDM are depicted in Fig. 6, whereby 2 subcarriers are modulated by the inner 16-QAM, while the other 2 subcarriers are modulated by the outer 16-QAM in each OFDM subblock. Therefore, a total of $g_1 + g_2 = 18$ information bits are transmitted per OFDM subblock, yielding the spectral efficiency of 4 bits/s/Hz. For its OFDM-IM counterpart, to reach the same spectral efficiency as DM-OFDM, 256-QAM is employed to modulate two subcarriers in each OFDM subblock, while the others are unmodulated. The $d_{\min}$ metrics for the DM-OFDM and OFDM-IM are $d_{\min,\mathrm{DM-OFDM}} = 0.8944$ and $d_{\min,\mathrm{OFDM-IM}} = 0.4339$. Since the ratio of $d_{\min,\mathrm{DM-OFDM}}$ to $d_{\min,\mathrm{OFDM-IM}}$ is considerably larger than that of *Example 1*, the performance gain of the DM-OFDM over the OFDM-IM is expected to be significantly higher for *Example 2*.

Since the computational complexity of both DM-OFDM associated with the ML detector and of OFDM-IM using the ML detector is on the order of $\mathcal{O}(262144)$ per subblock in terms of complex multiplications, the ML detection is difficult to implement in practice. However, in order to demonstrate that the performance of the reduced-complexity LLR detector is indistinguishable from that of the ML based detector for sufficiently high SNRs, we implemented both the ML based detector and the LLR based detector for DM-OFDM in our Monte Carlo simulations. Note that the DM-OFDM using the LLR based detector has a complexity on the order of $\mathcal{O}(128)$ per subblock, while OFDM-IM using the LLR based detector has a complexity on the order of $\mathcal{O}(512)$, which is considerably higher than that of DM-OFDM employing the LLR based detector. Fig. 7 portrays our BER performance comparison of DM-OFDM and OFDM-IM, where it can be seen that at the BER level of 10^{-3}, the DM-OFDM scheme relying on our LLR based detector achieves SNR gains of 6 dB and 5 dB over OFDM-IM using the LLR based detector for the AWGN and frequency-selective Rayleigh fading channels respectively, since two 16-QAM constellation sets are invoked by the DM-OFDM, which is naturally more robust both to noise and to interference than OFDM-IM in conjunction with 256-QAM. These large gains are particularly remarkable, considering the fact that in this high spectral efficiency case, the DM-OFDM combined with the LLR based detector actually has a lower complexity than the OFDM-IM with the LLR based detector. The results of Fig. 7 also confirm that the performance loss of the

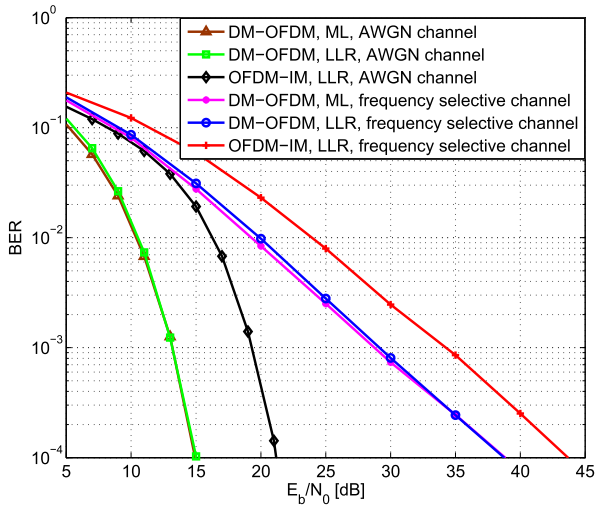

FIGURE 7. Performance comparison between DM-OFDM and OFDM-IM under both AWGN and frequency-selective Rayleigh fading channel conditions for *Example 2* with the spectral efficiency of 4 bits/s/Hz.

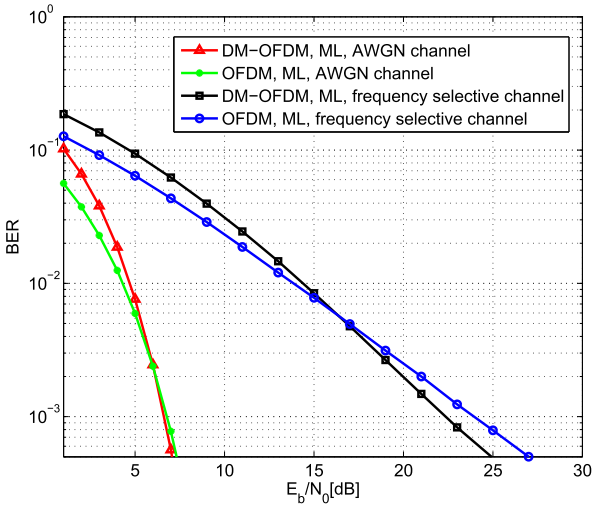

FIGURE 8. Performance comparison between DM-OFDM of 1.33 bits/s/Hz and OFDM-IM of 0.89 bits/s/Hz for *Example 3*.

DM-OFDM using the LLR detector in comparison to the DM-OFDM employing the ML detector is negligible even at low SNRs. Therefore, the reduced-complexity LLR detector is extremely attractive for DM-OFDM systems designed for a high spectral efficiency for its near ML performance and dramatically reduced complexity.

Example 3: To demonstrate the superiority of the proposed DM-OFDM over conventional OFDM, two BPSK constellation sets are adopted in DM-OFDM, which are defined as $\mathcal{M}_A = \{1, -1\}$ and $\mathcal{M}_B = \{\mathrm{j}, -\mathrm{j}\}$. In each OFDM subblock, two subcarriers are modulated by the mapper A, whilst the other subcarriers are modulated by the mapper B. Hence the number of total transmitted bits per subblock is 6, yielding the spectral efficiency of 1.33 bits/s/Hz. For the conventional OFDM counterpart, BPSK are employed for modulation, and the spectral efficiency is equal to 0.89 bits/s/Hz.

The performance of the proposed DM-OFDM is compared with the conventional OFDM counterpart in Fig. 8, where both the frequency-selective Rayleigh fading channel and the AWGN channel are considered. It can be seen that the performances of DM-OFDM and the conventional OFDM are almost the same at the BER level of 10^{-3} under AWGN channel assumptions, and the proposed DM-OFDM achieves more than 2dB performance gain over its OFDM counterpart under the frequency-selective channel besides its 0.44 bit/s/Hz spectral efficiency gain over OFDM. This is because higher spectral efficiency can reduce E_b, leading to smaller E_b/N_0 to attain certain BER. Therefore, it is demonstrated that the proposed DM-OFDM is capable of enhancing the performance of OFDM and conventional OFDM-IM.

Fig. 9 compares the PEP analysis of DM-OFDM using ML detection of *Example 3* to the simulated BER performance of DM-OFDM for a frequency-selective Rayleigh fading channel at the spectral efficiency of 1.33 bits/s/Hz. Like in *Example 1*, at high SNRs, the PEP analysis becomes accurate, as confirmed by the simulated BER.

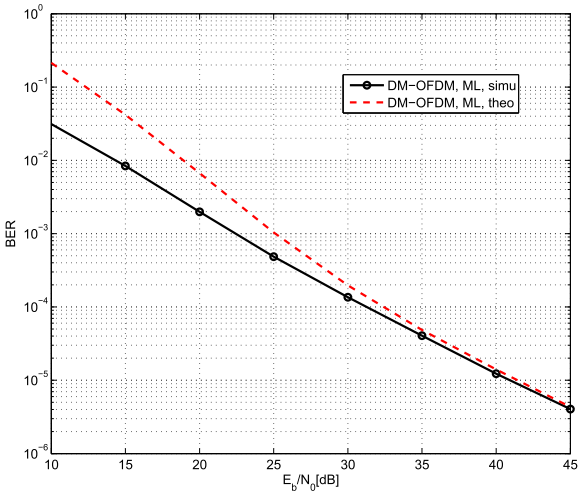

FIGURE 9. Comparison between the theoretical PEP analysis and the simulated BER performance for DM-OFDM under the frequency-selective Rayleigh fading channel of *Example 3*.

Additionally, the theoretical performance based on the PEP analysis of the DM-OFDM under AWGN channel conditions is also compared with its simulated counterpart for *Example 1* and *Example 3*, which is illustrated in Fig. 10. It can be seen that, despite the slight performance gap at low SNRs, the theoretical BER results are almost the same as the simulated counterparts at the SNR of 6dB and 10dB at the spectral efficiency of 1.33 bits/s/Hz and 2.22 bits/s/Hz respectively, which are achievable for practical DM-OFDM systems. It is indicated that the PEP analysis under the AWGN channel is more accurate than that of the frequency-selective Rayleigh fading channel condition. This is mainly because the FD channel coefficients are all one under the AWGN channel, and the UPEP can be directly calculated by (26), without the need of taking the approximation of (29), hence reducing the deviations compared with the PEP analysis under the frequency-selective Rayleigh fading channel.

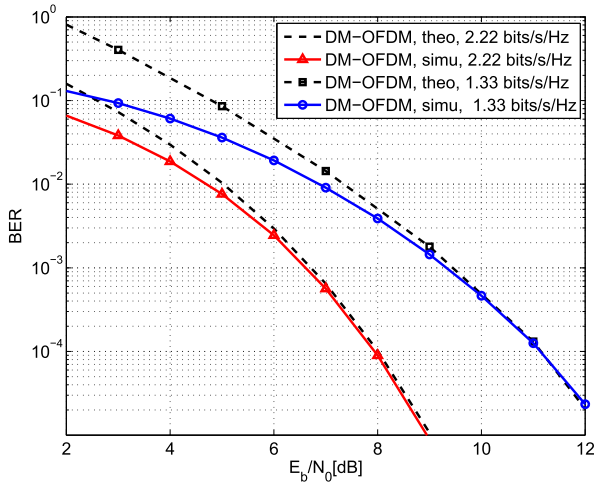

FIGURE 10. Comparison between the theoretical PEP analysis and the simulated BER performance for DM-OFDM under the AWGN channel of *Example 1* and *Example 3*.

V. CONCLUSIONS

In this paper, a novel DM-OFDM design has been proposed, whereby the subcarriers are divided into OFDM subblocks and the index modulation technique is applied. However, in contrast to the existing index-modulation-based OFDM, all the subcarriers are modulated, which improves the spectral efficiency. Specifically, at the transmitter, the subcarriers of each subblock are split into two groups, which are modulated by a pair of distinguishable modulation constellations, respectively. Thus, information bits are conveyed not only by the constellation symbols, but also by the subcarrier indices indicating the constellation modes of the subcarriers. At the receiver, a ML based detector and a reduced-complexity near optimal LLR based detector have been employed to demodulate the information bits by processing the received signals in the frequency domain. The minimum distance for different realizations of OFDM subblocks has been calculated, which demonstrates that the proposed DM-OFDM outperforms the conventional OFDM-IM, given the same spectral efficiency. Furthermore, the PEP analysis has been performed to estimate the BER of DM-OFDM. The Monte Carlo simulation results obtained have validated the theoretical analytical results and have also confirmed that DM-OFDM is capable of achieving a considerably better BER performance than its conventional OFDM-IM counterpart, while imposing the same or lower computational complexity, given the same spectral efficiency. The results have also confirmed that the performance of the DM-OFDM with the LLR based detector is indistinguishable from that of the DM-OFDM with the ML detector when the system's SNR is sufficiently high.

In this paper, we restrict our work on the transceiver design of the proposed DM-OFDM and the corresponding performance analysis. In the future study, we will consider index modulation techniques using tri-mode or quad-mode constellations, where three or four distinguishable constellation sets are employed for each OFDM subblock, and the throughput can be significantly enhanced. Moreover, we will also investigate the optimization of the size of OFDM subblocks and the constellation design of DM-OFDM, further improving the BER performance.

REFERENCES

[1] G. Zhang, M. De Leenheer, A. Morea, and B. Mukherjee, "A survey on OFDM-based elastic core optical networking," *IEEE Commun. Survey Tuts.*, vol. 15, no. 1, pp. 65–87, 1st Quart., 2013.

[2] L. L. Hanzo, M. Münster, B. J. Choi, and T. Keller, *OFDM and MC-CDMA for Broadband Multi-User Communications, WLANs and Broadcasting*. New York, NY, USA: Wiley, Jul. 2003.

[3] L. Hanzo and T. Keller, "Introduction to orthogonal frequency division multiplexing," in *OFDM MC-CDMA: A Primer*, 1st ed. New York, NY, USA: Wiley, 2006.

[4] M. Di Renzo, H. Haas, A. Ghrayeb, S. Sugiura, and L. Hanzo, "Spatial modulation for generalized MIMO: challenges, opportunities, and implementation," *Proc. IEEE*, vol. 102, no. 1, pp. 56–103, Jan. 2014.

[5] R. Mesleh, H. Haas, C. W. Ahn, and S. Yun, "Spatial modulation—A new low complexity spectral efficiency enhancing technique," in *Proc. CHINACOM*, Oct. 2006, pp. 1–5.

[6] R. Y. Mesleh, H. Haas, S. Sinanovic, C. W. Ahn, and S. Yun, "Spatial modulation," *IEEE Trans. Veh. Technol.*, vol. 57, no. 4, pp. 2228–2241, Jul. 2008.

[7] R. Fan, Y. J. Yu, and Y. L. Guan, "Generalization of orthogonal frequency division multiplexing with index modulation," *IEEE Trans. Wireless Commun.*, vol. 14, no. 10, pp. 5350–5359, Oct. 2015.

[8] Y. Xiao, S. Wang, L. Dan, X. Lei, P. Yang, and W. Xiang, "OFDM with interleaved subcarrier-index modulation," *IEEE Commun. Lett.*, vol. 18, no. 8, pp. 1447–1450, Aug. 2014.

[9] E. Basar, "Index modulation techniques for 5G wireless networks," *IEEE Commun. Mag.*, vol. 54, no. 7, pp. 168–175, Jul. 2016.

[10] R. Abu-Alhiga and H. Haas, "Subcarrier-index modulation OFDM," in *Proc. 20th IEEE Int. Symp. Indoor Mobile Radio Commun.*, Tokyo, Japan, Sep. 2009, pp. 177–181.

[11] D. Tsonev, S. Sinanovic, and H. Haas, "Enhanced subcarrier index modulation (SIM) OFDM," in *Proc. IEEE GLOBECOM Workshops*, Houston, TX, USA, Dec. 2011, pp. 728–732.

[12] E. Başar, U. Aygölü, E. Panayırcı, and H. V. Poor, "Orthogonal frequency division multiplexing with index modulation," *IEEE Trans. Signal Process.*, vol. 61, no. 22, pp. 5536–5549, Nov. 2013.

[13] E. Başar, "OFDM with index modulation using coordinate interleaving," *IEEE Wireless Commun. Lett.*, vol. 4, no. 4, pp. 381–384, Aug. 2015.

[14] E. Başar, "Multiple-input multiple-output OFDM with index modulation," *IEEE Signal Process. Lett.*, vol. 22, no. 12, pp. 2259–2263, Dec. 2015.

[15] E. Başar, "On multiple-input multiple-output OFDM with index modulation for next generation wireless networks," *IEEE Trans. Signal Process.*, vol. 64, no. 15, pp. 3868–3878, Aug. 2016.

[16] M. Wen, X. Cheng, L. Yang, Y. Li, X. Cheng, and F. Ji, "Index modulated OFDM for underwater acoustic communications," *IEEE Commun. Mag.*, vol. 54, no. 5, pp. 132–137, May 2016.

[17] X. Cheng, M. Wen, L. Yang, and Y. Li, "Index modulated OFDM with interleaved grouping for V2X communications," in *Proc. IEEE Int. Conf. Intell. Transp. Syst.*, Qingdao, China, Oct. 2014, pp. 1097–1104.

[18] Y. Ko, "A tight upper bound on bit error rate of joint OFDM and multicarrier index keying," *IEEE Commun. Lett.*, vol. 18, no. 10, pp. 1763–1766, Oct. 2014.

[19] M. Wen, X. Cheng, and L. Yang, "Optimizing the energy efficiency of OFDM with index modulation," in *Proc. IEEE Int. Conf. Commun. Syst.*, Macau, China, Nov. 2014, pp. 31–35.

[20] W. Li, H. Zhao, C. Zhang, L. Zhao, and R. Wang, "Generalized selecting sub-carrier modulation scheme in OFDM system," in *Proc. IEEE ICC Workshops*, Sydney, NSW, Australia, Jun. 2014, pp. 907–911.

[21] N. Ishikawa, S. Sugiura, and L. Hanzo, "Subcarrier-index modulation aided OFDM—Will it work?" *IEEE Access*, vol. 4, pp. 2580–2593, Jun. 2016.

[22] X. Yang, Z. Zhang, P. Fu, and J. Zhang, "Spectrum-efficient index modulation with improved constellation mapping," in *Proc. IEEE HMWC*, Xi'an, China, Oct. 2015, pp. 91–95.

[23] B. Zheng, F. Chen, M. Wen, F. Ji, H. Yu, and Y. Liu, "Low-complexity ML detector and performance analysis for OFDM with in-phase/quadrature index modulation," *IEEE Commun. Lett.*, vol. 19, no. 11, pp. 1893–1896, Nov. 2015.

[24] J. Erfanian, S. Pasupathy, and G. Gulak, "Reduced complexity symbol detectors with parallel structure for ISI channels," *IEEE Trans. Commun.*, vol. 42, nos. 2–4, pp. 1661–1671, Feb./Apr. 1994.
[25] W. Koch and A. Baier, "Optimum and sub-optimum detection of coded data disturbed by time-varying intersymbol interference," in *Proc. IEEE GLOBECOM*, San Diego, CA, USA, Dec. 1990, pp. 1679–1684.
[26] J. Li, M. Wen, X. Cheng, Y. Yan, S. Song, and M. Lee, "Generalised precoding aided quadrature spatial modulation," *IEEE Trans. Veh. Technol.*, vol. pp, no. 99, pp. 1–5, May 2016.
[27] M. Wen, Y. Li, X. Cheng, and L. Yang, "Index modulated OFDM with ICI self-cancellation in underwater acoustic communications," in *Proc. IEEE Asilomar Conf. Signals, Syst., Comput.*, Pacific Grove, CA, USA, Nov. 2014, pp. 338–342.
[28] M. Chiani and D. Dardari, "Improved exponential bounds and approximation for the Q-function with application to average error probability computation," in *Proc. IEEE GLOBECOM*, Taipei, China, Nov. 2002, pp. 1399–1402.
[29] R. A. Horn and C. R. Johnson, *Matrix Analysis*. Cambridge, U.K.: Cambridge Univ. Press, 1985.

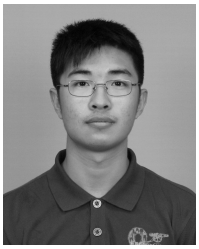

TIANQI MAO (S'15) received the B.S. degree from Tsinghua University, Beijing, China, in 2015, where he is currently pursuing the M.S. degree with the Department of Electronic Engineering. His current research interests include optical wireless communications and channel coding and modulation.

ZHAOCHENG WANG (M'09–SM'11) received the B.S., M.S., and Ph.D. degrees from Tsinghua University, Beijing, China, in 1991, 1993, and 1996, respectively. From 1996 to 1997, he was a Post-Doctoral Fellow with Nanyang Technological University, Singapore. From 1997 to 1999, he was with OKI Techno Centre (Singapore) Pte. Ltd., Singapore, where he was first a Research Engineer and later became a Senior Engineer. From 1999 to 2009, he was with Sony Deutschland GmbH, where he was first a Senior Engineer and later became a Principal Engineer. He is currently a Professor of Electronic Engineering with Tsinghua University and serves as the Director of Broadband Communication Key Laboratory and Tsinghua National Laboratory for Information Science and Technology. He has authored or coauthored over 100 journal papers (SCI indexed). He holds 34 granted U.S./EU patents. He co-authored two books, one of which entitled *Millimeter Wave Communication Systems* (Wiley-IEEE Press) was selected by the IEEE Series on Digital and Mobile Communication. His research interests include wireless communications, visible light communications, millimeterwave communications, and digital broadcasting. He is a fellow of the Institution of Engineering and Technology. Currently, he serves as an Associate Editor of the IEEE TRANSACTIONS on WIRELESS COMMUNICATIONS and the IEEE COMMUNICATIONS LETTERS, and has also served as Technical Program Committee Co-Chair of various international conferences.

QI WANG (S'15-M'16) received the B.E. degree and the Ph.D. degree (Hons.) in electronic engineering from Tsinghua University, Beijing, China, in 2011 and 2016, respectively. From 2014 to 2015, he was a Visiting Scholar with the Electrical Engineering Division, Centre for Photonic Systems, Department of Engineering, University of Cambridge. He has authored over 20 journal papers. His research interests include channel coding, modulation, and visible light communications. He was a recipient of the Outstanding Ph.D. Graduate of Tsinghua University, Excellent Doctoral Dissertation of Tsinghua University, National Scholarship, and the Academic Star of Electronic Engineering Department in Tsinghua University.

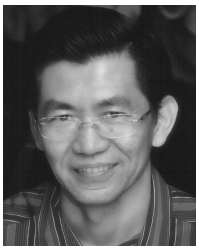

SHENG CHEN (M'90–SM'97–F'08) received the B.Eng. degree in control engineering from the East China Petroleum Institute, Dongying, China, in 1982, the Ph.D. degree in control engineering from City University, London, in 1986, and the D.Sc. degree from the University of Southampton, Southampton, U.K., in 2005. He held research and academic appointments with the University of Sheffield, the University of Edinburgh, and the University of Portsmouth, U.K., from 1986 to 1999. Since 1999, he has been with the Electronics and Computer Science Department, University of Southampton, where he is a Professor of Intelligent Systems and Signal Processing. He is also a Distinguished Adjunct Professor with King Abdulaziz University, Jeddah, Saudi Arabia. He has authored over 550 research papers. He was an ISI Highly Cited Researcher in engineering in 2004. His research interests include adaptive signal processing, wireless communications, modeling and identification of nonlinear systems, neural network and machine learning, intelligent control system design, evolutionary computation methods, and optimization. He is a fellow of IET. He was elected to a fellow of the United Kingdom Royal Academy of Engineering in 2014.

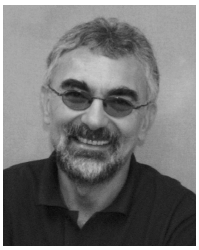

LAJOS HANZO (F'04) received the D.Sc. degree in electronics in 1976, the Ph.D. degree in 1983, and the Doctor Honoris Causa degree from the Technical University of Budapest in 2009. He also received the Ph.D. degree (Hons.) from the University of Edinburgh in 2015. During his 40-year career in telecommunications, he has held various research and academic positions in Hungary, Germany, and the U.K. From 2008 to 2012, he was the Editor-in-Chief of the IEEE Press and a Chaired Professor with Tsinghua University, Beijing. Since 1986, he has been with the School of Electronics and Computer Science, University of Southampton, U.K., as the Chair in Telecommunications. He has successfully supervised 110 Ph.D. students, co-authored 20 John Wiley/IEEE Press books in mobile radio communications totaling in excess of 10 000 pages, authored over 1500 research entries at the IEEE Xplore. He has over 25 000 citations. He is directing a 100 Strong Academic Research Team, working on a range of research projects in the field of wireless multimedia communications sponsored by the industry, the Engineering and Physical Sciences Research Council, U.K., the European Research Councils Advanced Fellow Grant, and the Royal Societys Wolfson Research Merit Award. He is an enthusiastic supporter of industrial and academic liaison and offers a range of industrial courses. He is also a fellow of the Royal Academy of Engineering, the Institution of Engineering and Technology, and the European Association for Signal Processing. He is a Governor of the IEEE VTS. He acted as the TPC Chair and General Chair of the IEEE conferences, presented keynote lectures, and received a number of distinctions.